

## Gyrokinetic modelling of stationary electron and impurity profiles in tokamaks

D. Tegnered<sup>1</sup>, A. Skyman<sup>1</sup>, H. Nordman<sup>1</sup>, P. Strand<sup>1</sup>

<sup>1</sup> *Department of Earth and Space Sciences, Chalmers University of Technology, SE-412 96  
Gothenburg, Sweden*

### Introduction

In order to optimize the performance of fusion devices the main ion profiles need to be peaked, since it enhances the fusion power production, while the impurity profiles should be hollow in order to minimize fuel dilution and radiation losses. Peaked profiles, in the absence of particle sources in the core, are then the result of an inward pinch caused by turbulent transport. Stationary profiles result from a balance of diffusion and convection resulting in zero particle flux. Since the electron density gradient can greatly affect the stationary impurity profile scaling,<sup>4</sup> a self-consistent treatment is used whereby the stationary local profiles corresponding to zero particle flux are calculated simultaneously for both electrons and trace impurities, as opposed to using a prescribed electron density gradient. Impurities with a charge  $3 \leq Z \leq 42$  are mainly included in trace amounts ( $n_Z/n_e = 10^{-6}$ ), so as not to affect the turbulent dynamics. The scaling of these profiles with regard to magnetic shear, safety factor, electron-to-ion temperature ratio, collisionality, toroidal sheared rotation, triangularity and elongation is discussed for a deuterium (D) plasma. Particle transport due to Ion Temperature Gradient (ITG) and Trapped Electron (TE) mode turbulence is studied using the gyrokinetic code GENE.<sup>1</sup> Quasilinear (QL) and nonlinear (NL) simulations are performed for parameters taken from the Cyclone Base Case,<sup>2</sup> an ITG dominated scenario. The gyrokinetic results are compared with results from a computationally efficient fluid model.<sup>3</sup> The simulations have been performed in a circular equilibrium with aspect ratio  $R/a = 3$ , using kinetic ions, electrons and impurities, except when studying the effects of shaping. Then the Miller equilibrium model was used.<sup>6</sup> The dynamics were further assumed to be electrostatic ( $\beta \approx 0$ ).

The local particle transport for species  $j$  can be formally divided into its diagonal and off-diagonal parts

$$\frac{R\Gamma_j}{n_j} = D_j \frac{R}{L_{n_j}} + D_{T_j} \frac{R}{L_{T_j}} + RV_{p,j}. \quad (1)$$

Here, the first term on the right hand side is the diffusion and the second and third constitute the off-diagonal pinch. The first of the pinch terms is the particle transport due to the

temperature gradient (thermo-diffusion) and the second is the convective velocity, which includes contributions from curvature, parallel compression and roto-diffusion. In equation (1),  $R/L_{X_j} \equiv -R\nabla X_j/X_j$  are the local gradient scale lengths of density and temperature, normalised to the major radius ( $R$ ). In general, the transport coefficients dependent on the gradients, though in the trace impurity limit the transport is linear in both  $R/L_{n_z}$  and  $R/L_{T_z}$ .

At steady state, the contributions from the different terms in the particle transport will tend to cancel, resulting in zero particle flux. Solving equation (1) for zero particle flux, with  $V_j = D_{T_j}1/L_{T_j} + V_{p,j}$  yields

$$PF_j \equiv \left. \frac{R}{L_{n_j}} \right|_{\Gamma=0} = -\frac{RV_j}{D_j}, \quad (2)$$

which is the steady state gradient of zero particle flux for species  $j$ . This measure quantifies the balance between diffusion and convection, and gives a measure of how “peaked” the local density profile is at steady state. It is therefore referred to as the “peaking factor” and denoted  $PF_j$ .

In order to investigate the transport, NL GENE simulations were performed from which  $PF_e$  for the stationary electron profiles were calculated. The results were compared with QL results, also obtained using GENE. The background peaking factor was found by explicitly seeking the gradient of zero particle flux by calculating the electron flux for several values of the density gradient. A typical set of simulations is displayed in Figure 1. The total flux is zero due to a balance of inward and outward transport occurring at different wavenumbers. This makes the reduced models sensitive to the choice of wavenumber. The method for finding  $PF_e$  from the QL simulations is the same, but here a reduced treatment was used, including only the dominant mode, which is an ITG mode for CBC-like parameters.

When finding the simultaneous peaking factor of the background and impurities, the former can be found first and used in the simulations of the latter without loss of generality, since the impurities are included in trace amounts. The peaking factors are calculated for several impurity species, using the reduced QL model.

### Simultaneous stationary profiles of electrons and impurities

First, we examine the dependence of the transport and of  $PF_e$  on the ion temperature gradient.

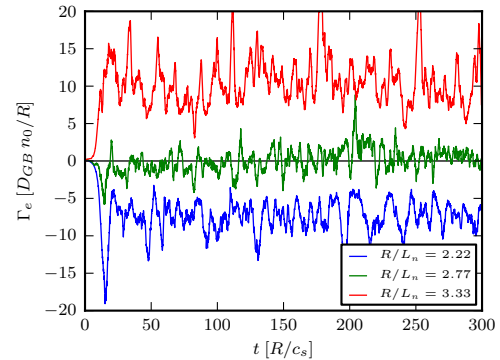


Figure 1: *Electron particle flux for different density gradients*

The result is shown in Figure 2, where the ion energy transport from NL simulations is displayed, together with electron peaking factors from NL, QL gyrokinetic and fluid simulations. In the TE mode dominated region ( $R/L_{T_i} \lesssim 5.0$ ), the peakedness of the background profile shows a steady increase with increasing ion temperature gradient, while the ion heat transport channel is small until the ITG mode is destabilised. Though the ion energy transport shows a stiff increase with the driving gradient above the ITG threshold, only a moderate reduction is seen in the peaking factor.<sup>7</sup> The addition of a 3% Beryllium background lowers the stiffness of the ion heat transport. The QL peaking factor shows a stronger decrease than its NL counterpart.

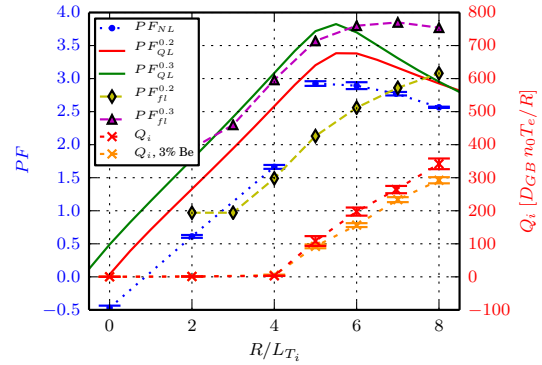


Figure 2: Scaling of  $PF_E$  and ion heat flux with ion temperature gradient

In Figure 3, the scaling with magnetic shear ( $\hat{s}$ ) is shown. The electron peaking shows a strong and near linear dependence on  $\hat{s}$ . This is the shear dependence of the curvature pinch. This trend is as strong in both the QL and NL simulations. The self-consistent results are shown in Figure 4. For the impurities, the change in peaking factors due to magnetic shear follows the trend seen for the electrons, and impurities with higher  $Z$  are more strongly affected. This is mainly due to a stronger inward convective pinch with increasing shear.

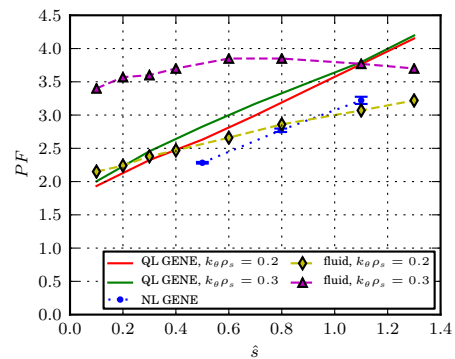


Figure 3: NL, QL, and fluid scalings of  $PF_e$  with magnetic shear

The electron peaking factor is reduced with both increasing ion-electron temperature ratio and collisionality,<sup>8</sup> in both the NL and QL simulations. With the selfconsistent treatment, the low- $Z$  impurities show the same trend while the high- $Z$  impurities are more flat, a result of the larger relative contribution of the outward thermopinch, which goes as  $1/Z$ .

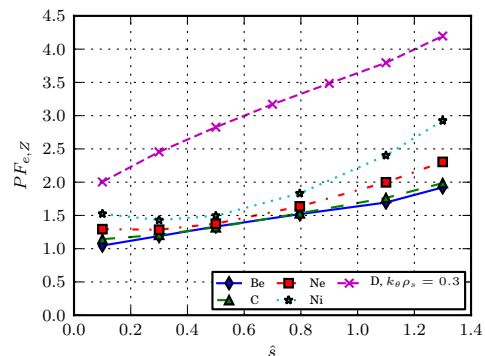


Figure 4: Simultaneous QL scalings of  $PF_e$  and  $PF_Z$ .

For elongation the QL electron peaking factor as well as the selfconsistent impurity factors increase with larger elongation. For low- $Z$  impurities the increase in peaking is mainly due to a larger inward thermopinch, while for high- $Z$  impurities it is caused by an increase in pure convection.

The fluid model reproduces most of the features of the gyrokinetic model as shown in Figure 2 and 3, though as with the QL model, the choice of wavenumber can be important.

For safety factor, sheared toroidal rotation and triangularity, the effects on the electron profile are weak and hence a selfconsistent treatment did not add significant new results to the previous investigations in this area.

### Conclusions

Reasonable qualitative agreement between NL, QL gyrokinetic, and fluid  $PF_e$  was found, but the reduced models were sensitive to the choice of wavenumber.  $PF_e$  was found to be sensitive in scans over temperature ratio, magnetic shear, collisionality, and elongation. It showed weak sensitivity for safety factor, sheared toroidal rotation, and triangularity. The selfconsistent treatment often resulted in similar trends for the background and the impurity peaking, so parameter regions with simultaneously high  $PF_e$  and low  $PF_Z$  are rare. Low collisionality was found to be favourable, since it allows for high  $PF_e$  with little effect on high-Z impurities.

### References

- [1] F Jenko, W Dorland, M Kotschenreuther, and B N Rogers. Electron temperature gradient driven turbulence. *Phys. Plasmas*, 7(5):1904, 2000.
- [2] A. M. Dimits, G. Bateman, M. A. Beer, B. I. Cohen, W. Dorland, G. W. Hammett, C. Kim, J. E. Kinsey, M. Kotschenreuther, A. H. Kritz, L. L. Lao, J. Mandrekas, W. M. Nevins, S. E. Parker, A. J. Redd, D. E. Shu-maker, R. Sydora, and J. Weiland. Comparisons and physics basis of tokamak transport models and turbulence simulations. *Phys. Plasmas*, 7(3):969, 2000.
- [3] J Weiland. *Collective Modes in Inhomogeneous Plasmas*. IoP Publishing, Bristol, UK, 2000.
- [4] A Skyman, H Nordman, and P Strand. Particle transport in density gradient driven TE mode turbulence. *Nucl. Fusion*, 52(11):114015, 2012.
- [5] F J Casson, A G Peeters, C Angioni, Y Camenen, W A Hornsby, A P Snodin, and G Szepesi. Gyrokinetic simulations including the centrifugal force in a rotating tokamak plasma. *Phys. Plasmas*, 17(10):102305, 2010.
- [6] R L Miller, M S Chu, J M Greene, Y R Lin-Liu, and R E Waltz. Noncircular, finite aspect ratio, local equilibrium model. *Phys. Plasmas*, 5(4):973, 1998.
- [7] E Fable, C Angioni, and O Sauter. The role of ion and electron electrostatic turbulence in characterizing stationary particle transport in the core of tokamak plasmas. *Plasma Phys. Contr. F.*, 52(1): 015007, 2010.
- [8] C Angioni, A G Peeters, F Jenko, and T Dannert. Collisionality dependence of density peaking in quasilinear gyrokinetic calculations. *Phys. Plasmas*, 12(11):112310, 2005.